Static and dynamic buckling of reconstructions at triple steps on Si(111) surfaces

ARTICLE *in* APPLIED PHYSICS LETTERS · OCTOBER 2014

Impact Factor: 3.3 · DOI: 10.1063/1.4900783

5 AUTHORS, INCLUDING:

Ruslan Zhachuk

Institute of Semiconductor Physics

33 PUBLICATIONS **220** CITATIONS

SEE PROFILE

S. A. Teys

Institute of Semiconductor Physics

71 PUBLICATIONS **493** CITATIONS

SEE PROFILE

J. Coutinho

University of Aveiro

128 PUBLICATIONS **1,250** CITATIONS

SEE PROFILE

Patrick R. Briddon

Newcastle University

490 PUBLICATIONS **8,832** CITATIONS

SEE PROFILE

Static and dynamic buckling of reconstructions at triple steps on Si(111) surfaces

R. Zhachuk, S. Teys, J. Coutinho, M. J. Rayson, and P. R. Briddon

Citation: Applied Physics Letters **105**, 171602 (2014); doi: 10.1063/1.4900783
View online: http://dx.doi.org/10.1063/1.4900783
View Table of Contents: http://scitation.aip.org/content/aip/journal/apl/105/17?ver=pdfcov
Published by the AIP Publishing

Static and dynamic buckling of reconstructions at triple steps on Si(111) surfaces

R. Zhachuk,[1,a)] S. Teys,[1] J. Coutinho,[2] M. J. Rayson,[3] and P. R. Briddon[4]
[1]*Institute of Semiconductor Physics, pr. Lavrentyeva 13, Novosibirsk 630090, Russia*
[2]*Department of Physics & I3N, University of Aveiro, Campus Santiago, 3810-193 Aveiro, Portugal*
[3]*Department of Chemistry, University of Surrey, Guildford GU2 7XH, United Kingdom*
[4]*School of Electrical, Electronic and Computer Engineering, Newcastle University, Newcastle Upon Tyne NE1 7RU, United Kingdom*

(Received 3 July 2014; accepted 19 October 2014; published online 29 October 2014)

Triple steps on Si(111) surfaces are popular building blocks for bottom-up nanostructure assembly, conferring size uniformity and precise positioning of growing nanostructures. In this work, we employ the Si(7 7 10) regular stepped surface as model system to study the triple steps by scanning tunneling microscopy (STM) and large-scale first-principles calculations. We find a surprising cohabitation of reconstruction elements at the step edge that either buckles statically or dynamically at room temperature. The driving force for the observed sequence of buckling patterns is traced back to Coulomb interactions involving charged adatoms and rest-atoms lying on a mini-terrace. These results reconcile the Si(111) triple step model with the experimental STM data. [http://dx.doi.org/10.1063/1.4900783]

Fabrication of nanoscale device structures requires a bottom-up approach based on self-assembly. Unlike lithography-based top-down routes, feature sizes can be ultimately shrunk down to the single-atom length scale. However, serious challenges remain in this field such as size fluctuations and positioning inaccuracy of self-assembled structures. In this respect, templates based on highly ordered stepped surfaces stand as promising structures along the road to overcoming these difficulties.

Vicinal Si(111) surfaces inclined towards the $[\bar{1}\bar{1}2]$ direction show a combination of one- and three-bilayer high steps.[1] The fraction of triple steps increases with the tilt angle of the vicinal surface with respect to [111].[2] When the angle reaches about 10° off the [111] direction we find (7 7 10) oriented surfaces, almost exclusively made of regularly spaced triple steps separated by (111) terraces showing a 7×7 dimer adatoms stacking fault (DAS) reconstruction.[3] Such stepped surface is unique from the structural point of view—unlike the steps on Si(100), terraces and step edges on Si(7 7 10) are all identical and straight, with a kink density of less than 25 μm^{-2}. Thanks to its structural perfection, the Si(7 7 10) surface with regular triple steps has served as template for growth of nanostructure arrays based on many different materials (see, for instance, Refs. 4 and 5). The observation of triple steps is not limited to vicinal Si(111) surfaces, they also show up during the initial stages of Si/Si(111) and Ge/Si(111) epitaxial island grow.[6,7] The $\langle\bar{1}\bar{1}2\rangle$ oriented triple steps define the Ge and Si island boundaries on Si(111) so that massive arrays of nanoislands of uniform three-bilayer thickness can be formed. Studies of strain fields in Si(111) stepped surfaces and quantum confinement of phonons in the aforementioned Ge islands were made possible thanks to the high uniformity of the structures formed.[6,8]

The frequent occurrence of triple steps on Si(111) implies a remarkably stable structure, most probably due to rebonding of Si dangling bonds at the triple step edge, effectively lowering the energy cost for step formation. In spite of the relevance of triples steps to the Si(111) surface landscape and nanostructure formation, its atomic structure is far from established.[9] The actual orientation of the regularly triple-stepped surface has been a matter of debate. While early reports on this subject indicated a (557) orientation [9.5° off the (111) plane], latter works report a (7 7 10) orientation [10.0° off the (111) plane].[3,10] Further, the triple step itself was ascribed to have (112), (113), and finally, no particular crystallographic orientation.[3,10,11]

Typical scanning tunneling microscopy (STM) images of the Si(7 7 10) are shown in Figs. 1(a) and 1(b). Over large areas of the sample surface, (111) terraces comprise exactly a single 7×7 unit cell, meaning that they naturally form a super-lattice of equidistant steps (within atomic accuracy). The prevailing model of the regularly triple stepped Si(7 7 10) has been proposed by some of us,[10] based on high resolution STM images and low energy electron diffraction data. The model is depicted in Fig. 1(c) and has recently received strong support from synchrotron radiation diffraction studies.[8]

In this letter, we present the first evidence that both static and dynamic buckling reconstruction elements coexist on the same Si(111) triple step. It is shown that the driving force behind the buckling of static elements arrives from interactions between charged atomic environments. Our starting point is the Si(7 7 10) atomic model shown in Fig. 1(c), which has received support from STM, low-energy electron diffraction, and synchrotron radiation diffraction (see Ref. 10 for further details). Accordingly, the periodicity of the (111) terrace is $\times 7$ along the $[\bar{1}10]$ step edge direction (as inherited from the (111)–7×7 DAS reconstruction), while the periodicity of reconstruction elements at the triple step edge is $\times 2$. The combined system (terrace plus step

[a)]Electronic mail: zhachuk@gmail.com

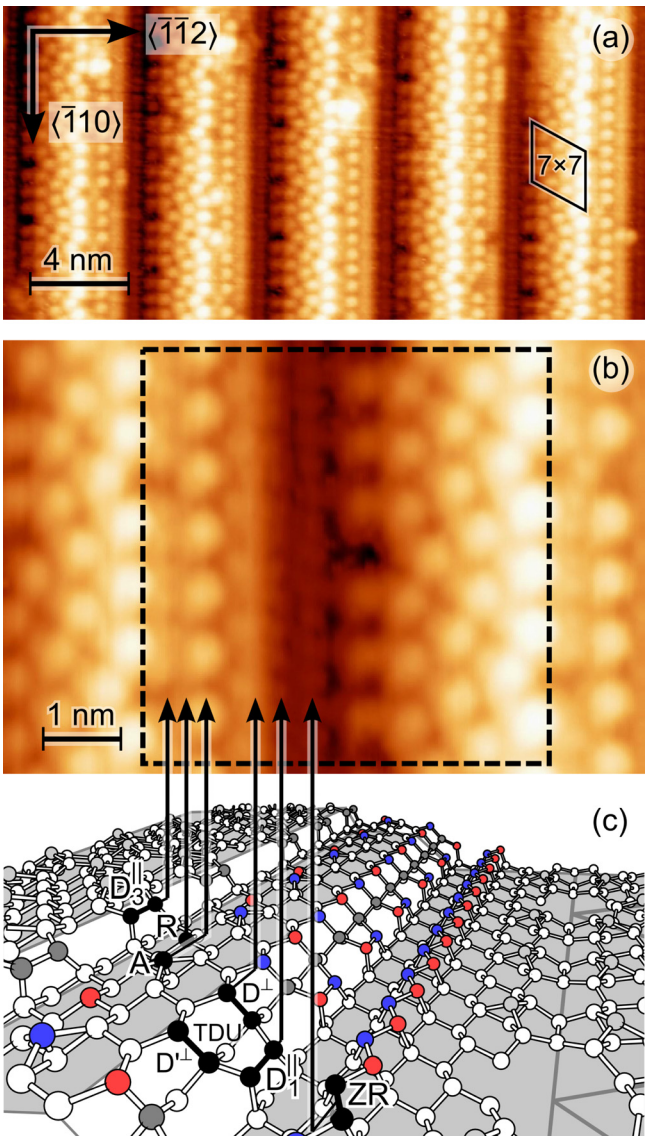

FIG. 1. (a) STM image of a clean Si(7 7 10) surface with regular triple steps. $U = +2.0$ V, $I = 23$ pA. (b) Close-up view of a triple step on Si(7 7 10). The simulated unit cell is outlined. $U = +1.0$ V, $I = 22$ pA. (c) Atomic model of the triple step, consisting of ZR-atoms forming a Seiwatz single-chain, TDUs comprising $D^{\perp}$, $D'\perp$, and $D_1^{\parallel}$ dimers, a (111) mini-terrace hosting adatoms (A) and rest-atoms (R), and $D_3^{\parallel}$ dimers at the edge of the (111) upper terrace. To make it perceptible to the eye, reconstruction elements are shown without asymmetric distortions. Red/blue colored atoms represent radicals that accept/donate electrons in the ground state.

edge) has therefore a $\times 14$ periodicity and spans two 7×7 unit cells. This corresponds to a remarkably large unit cell with $5.4 \times 5.4\,\text{nm}^2$ surface area as outlined in Fig. 1(b).

The surface model for the electronic structure calculations consisted on repeated slabs comprising a total of 2215 atoms (including saturating hydrogen atoms at the back side). Total energy and atomic relaxation calculations were carried out using the pseudopotential[12] density functional theory (DFT) AIMPRO code[13,14] within the local density approximation to the exchange and correlation interactions between electrons.[15] Potential terms and charge density were treated in reciprocal-space with plane-waves limited at a cut-off energy of 200 Ha. Valence states were expressed as linear combinations of Cartesian-Gaussian functions on Si (16 *sp*-like plus 12 *d*-like) and H (16 *sp*-like) and the Brillouin-zone was sampled at $\mathbf{k} = \Gamma$. Slab models consisted of four Si bilayers (in the (111) terrace and step edge regions) and the vacuum space that was at least 3.3 nm thick. The bottom Si layer was passivated by hydrogen and kept frozen during surface optimization. All remaining atoms were allowed to move until residual forces were less than 0.16 eV/nm. The relaxed coordinates were used to calculate the local density of states (LDOS) using the SIESTA density functional package,[16] using similar conditions to those in Ref. 17. The constant-current STM images were simulated within the Tersoff-Hamann approximation.[18,19]

STM images were recorded at room temperature in the constant-current mode using an electrochemically etched tungsten tip. The measurements were performed in ultra-high vacuum (9×10^{-11} Torr) on a system equipped with a STM (OMICRON). The samples were prepared as described in Ref. 3.

According to Fig. 1(c), the step edge comprises the following (black colored) reconstruction elements: A Seiwatz-like[20] zig-zag row (ZR) of atoms, triple dimer units (TDU), each made of two dimers perpendicular to the step edge ($D^{\perp}$ and $D'^{\perp}$) covalently bound to a dimer ($D_1^{\parallel}$) parallel to the edge, a Si(111) mini terrace hosting adatoms (A) and rest-atoms (R), and finally, a row of parallel dimers ($D_3^{\parallel}$) at the Si(111) terrace edge.[10]

We start by analyzing ZR atoms and TDUs. With the exception of the Si(7 7 10), ZR elements were never found in Si surfaces. They were suggested to take place on cleaved 2×1-reconstructed Si(111) and Ge(111),[21] but it was later shown that the π-bonded Pandey model (PM) chain agrees better with the observations.[22] Each ZR atom is threefold coordinated. The resulting alternating parallel radicals are prone to form π-bonded rows consistent with the Seiwatz chain model.[20] The symmetric atomic configuration, with all ZR atoms having identical sp^3-bonds, is unstable against buckling. The ZR atoms are not equivalent with respect to the (111) sub-surface atomic monolayer, i.e., their second neighbors. ZR atoms closer (farthest) to the step edge have one (two) second neighbor(s), respectively. Hence, we refer to $ZR_{C\uparrow,F\downarrow}$ as a configuration where atoms in rows closer (C) and farthest (F) to the step edge are, respectively, raised (↑)/dented (↓) with respect to the symmetric configuration. After atomic relaxation, we found $ZR_{C\downarrow,F\uparrow}$ to be the lowest energy configuration. Accordingly, ZR_F-atoms are raised, their three bonds become strongly *p*-like and a fully occupied dangling bond state, mostly *s*-like, is formed. Conversely, ZR_C-atoms are lowered to become approximately sp^2-coordinated. They produce high-energy *p*-like dangling bond states, whose electrons are donated to the *s*-type radicals on farthest ZR_F-atoms. This electron transfer is shown in Fig. 2(c). A high LDOS on ZR_C/ZR_F atoms is probed for empty/filled electronic states, respectively, and that matches the STM findings as shown in Fig. 2(a).

At the step edge, each $D_1^{\parallel}$-dimer binds to two perpendicular $D^{\perp}$ and $D'^{\perp}$ dimers, only distinguishable by the fact that $D^{\perp}$ is closer to an A-adatom sitting at the (111) mini-terrace. The three dimers within each TDU cannot flip independently. They comprise a total of four dangling bonds that can exchange charge upon complex buckling. $D_1^{\parallel}$-dimers have a similar atomic neighborhood to Si(100)–2×1 dimers. They

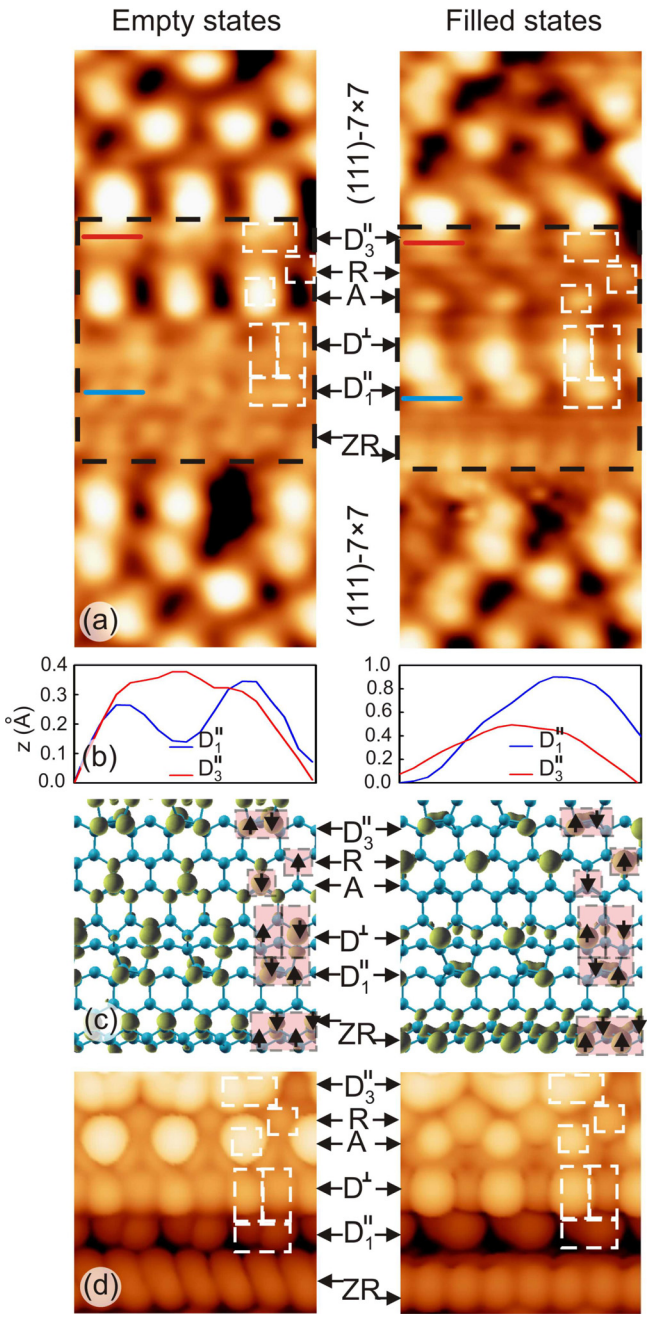

FIG. 2. (a) STM images of the triple step with two adjacent (111)-7 × 7 terraces measured with $I = 22$ pA and a bias $U = +1.0$ V (left) and $U = -1.4$ V (right). (b) Line scans across $D_1^{\parallel}$ and $D_3^{\parallel}$ dimers as represented by the blue and red segments in (a). (c) LDOS isosurfaces integrated across a 1 eV window above (left) and below (right) the calculated Fermi level. (d) STM images of the triple step simulated within the Tersoff-Hamann approximation (integrated over a 1 eV window). Black dashed lines in (a) outline the region of the triple step edge. White dashed lines highlight various reconstruction elements at the triple step. Up/down arrows indicate atoms shifted upwards/inwards and showing p^3-/sp^2-like bonding, respectively.

buckle like dimers in $c(4 \times 2)$ and $p(2 \times 2)$ reconstructions on Si(100). Here, one atom is raised (leading to a low-energy *s*-like dangling bond), the other is depressed (leading to a high-energy *p*-like dangling bond), and electron-transfer from the *p*-radical to the *s*-radical.[23,24] Such static asymmetry is clearly demonstrated by the blue line in Fig. 2(b), which represents height profiles of $D_1^{\parallel}$ line scans. $D^{\perp}$ and $D'^{\perp}$ dimers have their lower Si atoms chemically bound to $D_1^{\parallel}$ and their structures strongly depend on distortions at their $D_1^{\parallel}$ neighbors. This is demonstrated in Fig. 2(c), where buckling of $D_1^{\parallel}$ actually affects the charge transfer to and between $D^{\perp}$- and $D'^{\perp}$-dimer radicals within a TDU. Upon atomic relaxations, we found that lowered Si radicals in buckled $D_1^{\parallel}$-dimers lever their coupled $D^{\perp}$ (or $D'^{\perp}$) top radicals to become *knobbed*. Analogously, protrusion of a Si radical in $D_1^{\parallel}$ leads to the *indentation* of the top radical in $D'^{\perp}$ (or $D^{\perp}$) connected to it. This effect follows from an intrinsic *driving force* to keep the sp^3 bond lengths/angles across the Si network. We thus label a specific TDU structure by referring to a knobbed ($TDU_{\uparrow}$)/dented ($TDU_{\downarrow}$) state of the $D^{\perp}$-radical just opposite to the adatom A.

We relaxed and compared total energies of four buckled structures involving combinations of ZR and TDU structures. The ground state configuration is made of $ZR_{C\downarrow,F\uparrow}$ and $TDU_{\uparrow}$ (with a protruded $D^{\perp}$-radical) structures. The effect of flipping TDUs to the energy difference between $ZR_{C\downarrow,F\uparrow}$ and $ZR_{C\uparrow,F\downarrow}$ was only about 1.1 meV/nm^2. A similar result was found by tipping over ZR atoms when calculating the relative stability of $TDU_{\uparrow}$ and $TDU_{\downarrow}$. This indicates that coupling between ZR and TDUs is negligible and they can be considered independent. The $ZR_{C\downarrow,F\uparrow}$ configuration is energetically more favorable than $ZR_{C\uparrow,F\downarrow}$ by 17.8 meV/nm^2, while $TDU_{\uparrow}$ is more stable than $TDU_{\downarrow}$ by 8.5 meV/nm^2 (or 36 meV/TDU). Such small energy differences should be considered with care since they edge the error bar of the methods employed. We note however that they relate to configurations that are very similar, and therefore are expected to be qualitatively meaningful.

Figure 2(a) shows STM images of empty/filled electronic states of the triple step on Si(7 7 10) with two adjacent Si(111)–7 × 7 terraces. The ground state buckled configuration of Si(7 7 10) was used to generate LDOS plots and simulate constant-current STM images. These are depicted in Figs. 2(c) and 2(d), respectively. The simulated STM calculations employed a symmetric ±1 eV energy window and this allows an easier inspection of surface states that show different contrast on forward and reverse bias. A picture generated at −1.4 eV did not show any significant difference with respect to the one at −1.0 eV. When comparing experimental and simulated STM images based on DFT, two main aspects deserve special attention: (i) relative positions of local bright maxima (usually these point to surface atoms positions) and (ii) the variation of their brightness upon bias polarity change (that shows which atoms accept/donate electrons due to local bonding of surface atoms). The close correspondence regarding both aspects complements the total energy results, conferring further and compelling support to the atomic model in Fig. 1(c). We also note that any influence of the STM tip on the buckling configurations is very unlikely. Images were acquired at low tunneling current and at room temperature so that any injected charge from the STM tip should quickly dissipate into the Si bulk.

While the above results provide compelling support to the structure of the triple step model, we are left unanswered to why ZR and TDU elements prefer to buckle towards a particular direction. Adatoms and rest atoms at the (111) mini terrace are close enough to TDUs, so that they can break the local symmetry of the latter by coupling to $D^{\perp}$-dimers. Fig.

2(c) shows that electron transfer takes place from adatoms to rest atoms. This is also the case in 7×7, 2×2, and $c(2 \times 8)$ reconstructions on silicon and germanium (111) surfaces.[25] Adatoms become positively charged, whereas rest atoms become negatively charged, effectively stabilizing the $TDU_{\uparrow}$ state due to a Coulomb effect. The decisive role of adatoms in buckling of TDUs was confirmed after two additional surface calculations, where Si(7 7 10) surfaces with $TDU_{\uparrow}$ and $TDU_{\downarrow}$ states were further relaxed after removing A-adatoms from the (111) mini-terrace. Both final surfaces were identical and exhibited no TDU buckling at all, demonstrating that TDU buckling follows directly from adatom charging. Electrostatics may also explain the resulting ZR buckling direction. While ZR_F dangling-bonds overlap underlying hexagonal voids depleted of electrons, ZR_C-dangling bonds project over Si sites at the (111) terrace sub-monolayer. The energy of ZR_F-dangling bonds is therefore lowered (with respect to that of ZR_C -radicals) as they overlap with a lower electron density. It is noteworthy that this behavior also holds for ZR on flat Si(111)–2×1.

Now, we report on $D_3^{\parallel}$ dimers at the (111) upper terrace edge. These dimers are symmetric when they are part of 7×7 DAS structure on flat Si(111). The calculations show though, that when placed on the (111) terrace edge, these dimers are unstable against buckling [see Figs. 2(c) and 2(d)], in contrast with the STM image in Fig. 2(a) and the line scans in Fig. 2(b) (red lines), indicating that they are symmetric. This apparent contradiction was investigated by looking at a total of six step structures, where the buckling direction of $D_3^{\parallel}$ dimers was set differently. The calculations show that all relaxed structures are virtually degenerate, with their energies differing by at most 3 meV per flipped dimer. This is close to the reported interaction between nearest dimers in two adjacent dimer rows on Si(100).[24] The energy barrier for flipping a single $D_3^{\parallel}$ is only 35 meV high. This was obtained by relaxing seven intermediate images connected by a nudged elastic band between equivalent end-structures.[26] Such a small figure demonstrates that $D_3^{\parallel}$ dimers are able to flip at room temperature and that the above STM images effectively represent a symmetric time-averaged picture of the fast-flipping structures. STM imaging of $D_3^{\parallel}$ dimers at low temperature could provide further insight into the dynamic nature of their structures. We hope that our calculations will inspire others in pursuing such measurements using an appropriate STM setup.

In conclusion, from a combined large-scale DFT and STM study of the Si(7 7 10) regular stepped surface, we arrived at a detailed picture of the atomic structure of triple steps on Si(111) surfaces. The calculations support the model proposed in Ref. 10 [cf. Fig. 1(c)], suggesting that the triple step structure has no particular crystallographic orientation. We show that both static and dynamic buckling reconstruction elements coexist in Si(111) triple steps at room temperature. The $D_3^{\parallel}$ dimers at the edge of (111)–7×7 terraces flip at room temperature, while TDUs and Seiwatz-like ZR-atoms form static buckling patterns due to Coulomb interaction with their respective neighboring atomic environments. These two latter elements show a two-fold asymmetric buckling mode. TDU buckling depends on a complex many-body mechanism involving (i) electron-transfer from adatoms to rest-atoms, (ii) Coulomb stabilization of $TDU_{\uparrow}$ radicals by positively charged adatoms, and finally (iii) a relaxation of $D_1^{\parallel}$-dimers to minimize local sp^3 bond length/angle distortions. ZR buckling, on the other hand, is driven by Coulomb stabilization of ZR_F-radicals by the underlying electron density at the (111) terrace. The model is in agreement with the spectroscopic STM data, shedding light into the atomic and electronic details of the Si(111) triple step.

We would like to thank the Novosibirsk State University for providing the computational resources. This work was supported by Russian Foundation for Basic Research (Project No. 14-02-00181). J.C. thanks the FCT (Portugal) under the grants PTDC/CTM-ENE/1973/2012 and PEst-C/CTM/LA0025/2013 for funding.

[1]R. J. Phaneuf and E. D. Williams, Phys. Rev. B **41**, 2991 (1990).
[2]J. Wei, X.-S. Wang, J. L. Goldberg, N. C. Bartelt, and E. D. Williams, Phys. Rev. Lett. **68**, 3885 (1992).
[3]A. Kirakosian, R. Bennewitz, J. N. Crain, T. Fauster, J.-L. Lin, D. Y. Petrovykh, and F. J. Himpsel, Appl. Phys. Lett. **79**, 1608 (2001).
[4]C. Tegenkamp, T. Ohta, J. L. McChesney, H. Dil, E. Rothenberg, H. Pfnür, and K. Horn, Phys. Rev. Lett. **100**, 076802 (2008).
[5]R. A. Zhachuk, S. A. Teys, A. E. Dolbak, and B. Z. Olshanetsky, Surf. Sci. **565**, 37 (2004).
[6]S. Teys, A. Talochkin, and B. Olshanetsky, J. Cryst. Growth **311**, 3898 (2009).
[7]B. Voigtländer and M. Kastner, Appl. Phys. A **63**, 577 (1996).
[8]G. Prévot, F. Leroy, B. Croset, Y. Garreau, A. Coati, and P. Müller, Surf. Sci. **606**, 209 (2012).
[9]R. Zhachuk and S. Pereira, Phys. Rev. B **79**, 077401 (2009).
[10]S. A. Teys, K. N. Romanyuk, R. A. Zhachuk, and B. Z. Olshanetsky, Surf. Sci. **600**, 4878 (2006).
[11]M. Henzler and R. Zhachuk, Thin Solid Films **428**, 129 (2003).
[12]C. Hartwigsen, S. Goedecker, and J. Hutter, Phys. Rev. B **58**, 3641 (1998).
[13]M. J. Rayson and P. R. Briddon, Phys. Rev. B **80**, 205104 (2009).
[14]M. J. Rayson, Comput. Phys. Commun. **181**, 1051 (2010).
[15]J. P. Perdew and Y. Wang, Phys. Rev. B **45**, 13244 (1992).
[16]J. M. Soler, E. Artacho, J. D. Gale, A. García, J. Junquera, P. Ordejón, and D. Sánchez-Portal, J. Phys.: Condens. Matter **14**, 2745 (2002).
[17]R. Zhachuk, B. Olshanetsky, J. Coutinho, and S. Pereira, Phys. Rev. B **81**, 165424 (2010).
[18]I. Horcas, R. Fernandez, J. M. Gomez-Rodriguez, J. Colchero, J. Gomez-Herrero, and A. M. Baro, Rev. Sci. Instrum. **78**, 013705 (2007).
[19]J. Tersoff and D. R. Hamann, Phys. Rev. Lett. **50**, 1998 (1983).
[20]R. Seiwatz, Surf. Sci. **2**, 473 (1964).
[21]R. Feder, P. P. Auer, and W. Mönch, J. Phys. C **12**, L179 (1979).
[22]K. C. Pandey, Phys. Rev. Lett. **47**, 1913 (1981).
[23]S. J. Jenkins and G. P. Srivastava, J. Phys.: Condens. Matter **8**, 6641 (1996).
[24]A. Ramstad, G. Brocks, and P. J. Kelly, Phys. Rev. B **51**, 14504 (1995).
[25]A. A. Stekolnikov, J. Furthmüller, and F. Bechstedt, Phys. Rev. B **65**, 115318 (2002).
[26]G. Henkelman, B. P. Uberuaga, and H. Jónsson, J. Chem. Phys. **113**, 9901 (2000).